

tric filler. This is possibly due to the nonmonotonic change of coefficient of electron penetration through the barrier corresponding to the dielectric filler, which should lead to oscillations of the effective mean free path of the electrons.

In conclusion, the author thanks M. N. Mikheev for all-out help and constant interest, V. M. Golyanov for preparing the samples, M. B. Tsetlin for useful discussions, and E. A. Zhitnitskii for help with the measurements.

<sup>1</sup>This formula (at  $\eta = 1$ ) follows (see<sup>[18]</sup>) from Gor'kov's theory.<sup>[9]</sup> The coefficient  $\eta$  has been introduced to take into account possible tight-binding effects.

<sup>1</sup>M. N. Mikheeva, M. B. Tsetlin, A. A. Teplov, V. M. Golyanov, and A. P. Demidov, Pis'ma Zh. Eksp. Teor. Fiz. 15, 303 (1972) [JETP Lett. 15, 213 (1972)].

<sup>2</sup>V. M. Golyanov, M. N. Mikheeva, and M. B. Tsetlin, Zh. Eksp. Teor. Fiz. 68, 736 (1975) [Sov. Phys. JETP 41, 365 (1975)].  
<sup>3</sup>V. M. Golyanov and M. N. Mikheeva, Zh. Eksp. Teor. Fiz. 70, 2236 (1976) [Sov. Phys. JETP 43, (1976)].  
<sup>4</sup>H. Sixl, Phys. Lett. 53A, 333 (1975).  
<sup>5</sup>V. M. Golyanov, M. N. Mikheeva, A. P. Demidov, and A. A. Teplov, Zh. Eksp. Teor. Fiz. 58, 528 (1970) [Sov. Phys. JETP 31, 283 (1970)].  
<sup>6</sup>G. Bergmann, Phys. Rev. B7, 4850 (1973).  
<sup>7</sup>A. A. Teplov, M. N. Mikheeva, and V. M. Golyanov, Zh. Eksp. Teor. Fiz. 68, 1108 (1975) [Sov. Phys. JETP 41, 549 (1975)].  
<sup>8</sup>A. A. Teplov, M. N. Mikheeva, V. M. Golyanov, and A. N. Gusev, Zh. Eksp. Teor. Fiz. 71, No. 9 (1976) [Sov. Phys. JETP 44, No. 9 (1976)].  
<sup>9</sup>L. P. Gor'kov, Zh. Eksp. Teor. Fiz. 37, 1407 (1959) [Sov. Phys. JETP 10, 998 (1960)].

Translated by J. G. Adashko

## Turbulent mixing at contact surface accelerated by shock waves

V. A. Andronov, S. M. Bakhrakh, E. E. Meshkov, V. N. Mokhov, V. V. Nikiforov, A. V. Pevnitskii, and A. I. Tolshmyakov

(Submitted March 22, 1976)  
 Zh. Eksp. Teor. Fiz. 71, 806-811 (August 1976)

Turbulent mixing at a contact surface between two gases of different density which is accelerated by plane stationary normally-incident shock waves is observed experimentally. A system of equations describing the nonstationary turbulent flow of the compressed gases is proposed. Results are presented of numerical calculations of the experimental data on turbulent mixing of the contact surface between gases of different density following multiple passage of shock waves through the surface. Satisfactory agreement between the calculations and experiments can be attained by suitable choice of the empirical constants.

PACS numbers: 45.30.Jm, 45.40.Nx

It is known that the boundary between gases having different densities is unstable to small perturbations if the pressure and density gradients on the boundary are directed oppositely (the so-called gravitational instability), or else if a shock wave passes through the boundary. The development of small perturbations can lead to the onset of turbulence in the vicinity of the boundary, and accordingly to turbulent mixing of the gases.<sup>[1,2]</sup>

### 1. MODEL OF TURBULENT MIXING

To describe gasdynamic flow with allowance for the possible onset of turbulence and the ensuing turbulent mixing, we used the following system of equations:

$$d\rho/dt = -\rho \operatorname{div} \mathbf{v}, \quad (1)$$

$$\frac{d\mathbf{v}}{dt} = -\frac{1}{\rho} \nabla(P+P_t) + \frac{1}{\rho} \frac{\partial}{\partial x_k} [(v+v_t)\rho\sigma_{ik}], \quad (2)$$

$$\frac{dE}{dt} = \frac{P}{\rho^2} \frac{d\rho}{dt} - \frac{1}{\rho} \operatorname{div} \mathbf{q}_t + v\sigma_{ik} \frac{\partial v_i}{\partial x_k} - D_t \left( \kappa \nabla P - \frac{\nabla \rho}{\rho} \right) \frac{\nabla P}{\rho} + k_1 \left( 1 + k_2 \frac{v}{v_t} \right) \frac{\epsilon_t^2}{v_t}, \quad (3)$$

$$\frac{dc_i}{dt} = -\frac{1}{\rho} \operatorname{div} \mathbf{j}_{it}, \quad (4)$$

$$\frac{d\epsilon_t}{dt} = \frac{1}{\rho} \operatorname{div} \rho D_t \nabla \epsilon_t - \frac{1}{\rho} P_t \operatorname{div} \mathbf{v} + v_t \sigma_{ik} \frac{\partial v_i}{\partial x_k} + D_t \left( \kappa \nabla P - \frac{\nabla \rho}{\rho} \right) \frac{\nabla P}{\rho} - k_1 \left( 1 + k_2 \frac{v}{v_t} \right) \frac{\epsilon_t^2}{v_t}. \quad (5)$$

Here

$$\frac{d}{dt} = \frac{\partial}{\partial t} + (\mathbf{v} \nabla), \quad \sigma_{ik} = \frac{\partial v_i}{\partial x_k} + \frac{\partial v_k}{\partial x_i} - \frac{2}{3} \delta_{ik} \operatorname{div} \mathbf{v},$$

$\nu$  is the coefficient of kinematic viscosity,  $\nu_t$  is the coefficient of turbulent viscosity,  $D_t$  is the coefficient of turbulent diffusion,

$$\mathbf{q}_t = -\rho D_t \nabla \left( E + \frac{P}{\rho} \right)$$

is the turbulent heat flux,  $c_i$  is the concentration of the  $i$ -th component,  $\mathbf{j}_{it} = -\rho D_t \nabla c_i$  is the turbulent mass flux of the  $i$ -th component,  $\epsilon_t$  is the kinetic energy of the turbulence,  $P_t = \frac{2}{3} \rho \epsilon_t$  is the pressure increment due to  $\epsilon_t$ ,

$$\kappa = \lambda - \beta^2 T / \rho c_p,$$

where

$$\lambda = \frac{1}{\delta} \frac{\partial \rho}{\partial P} \Big|_{c_i, T}, \quad \beta = - \frac{1}{\rho} \frac{\partial \rho}{\partial T} \Big|_{c_i, P}, \quad c_p = T \frac{\partial S}{\partial T} \Big|_{c_i, P},$$

$k_1$  and  $k_2$  are constants.

Equations (1)–(4) are obtained from the widely used assumption that the turbulent flow is analogous to the flow of a viscous multicomponent liquid with certain effective turbulent coefficients of diffusion and viscosity. Equation (5) can be obtained from energy consideration (in analogy with<sup>[1]</sup>) and differs from the equation for  $\varepsilon_t$  in<sup>[1]</sup> by terms that take into account the non-isothermy, the inertia of the turbulence, the compressibility, and the diffusion of the turbulent energy. The expression for the rate of dissipation of the turbulent energy

$$k_1 \left( 1 + k_2 \frac{v}{v_t} \right) \frac{\varepsilon_t^2}{v_t}$$

is similar in form to that used in<sup>[3,4]</sup>. In the presence of shock waves, the value of the expression  $(\kappa \Delta P - \nabla \rho / \rho)$  in (3) and (5) must be taken ahead of the shock-wave front.

To make the system (1)–(5) a closed one, we must determine  $\nu_t$  and  $D_t$ . The simplest method, used in<sup>[1]</sup>, is to define  $\nu_t$  in the form

$$\nu_t = \alpha L \sqrt{\varepsilon_t} \quad (6)$$

where  $L$  is the width of the mixing zone, and  $\alpha$  is a constant. A shortcoming of this definition is that  $\alpha$  is different for different problems. Experience in the study of shear flow (see<sup>[3,4]</sup>) has shown that good agreement with the experimental data is obtained in a large class of problem by using more complicated differential equations for  $\nu_t$ . Starting from semi-qualitative considerations, we can obtain for  $\nu_t$  the equation

$$\frac{d\nu_t}{dt} = \frac{1}{\rho} \operatorname{div} \rho D_t \nabla \nu_t + \alpha_1 \frac{\nu_t^2}{\varepsilon_t} \sigma_{ik} \frac{\partial \nu_t}{\partial x_k} + \alpha_2 \frac{\nu_t^2}{\varepsilon_t} \left( \kappa \nabla P - \frac{\nabla \rho}{\rho} \right) \frac{\nabla P}{\rho} - 0.3 k_2 \frac{v}{\nu_t} \varepsilon_t, \quad (7)$$

where  $\alpha_1$  and  $\alpha_2$  are constants; the coefficient 0.3 in the last term ensures satisfaction of the correct laws for the damping of the isotropic turbulence. As to  $D_t$ , it is assumed that  $D_t = \nu_t / S_c$ , where  $S_c$  is the Schmidt number.

## 2. EXPERIMENTAL STUDY OF THE INSTABILITY OF A CONTACT SURFACE

Turbulent mixing on the boundary between two gases having different densities (the contact surface), when the

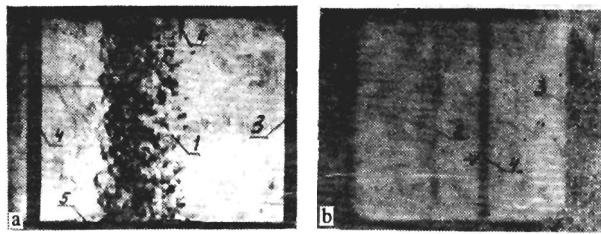


FIG. 2.

boundary is accelerated by plane stationary shock waves, was observed experimentally in the case of normal incidence of the waves.

The experiments were performed with a shock tube described in<sup>[5]</sup>, where a description of the experimental technique can also be found. The end of the shock-tube channel (see Fig. 1), with transparent side walls, consisted of two contiguous blocks 1 and 2, separated by a thin organic film 3 of thickness 0.3–0.5  $\mu$  and specific mass  $(3-4) \times 10^{-5}$  g/cm<sup>2</sup>. The end of the channel was sealed with a stopper. The closed volume 2 was filled with helium, while the remaining end of the channel was filled with air at atmospheric pressure. A plane stationary shock wave 5 with Mach number  $M = 1.3$ , produced in the shock tube, passed through the boundary 3 and accelerated the latter. After reflection from the rigid wall 4, the shock wave passed again through the contact surface in the opposite direction, was reflected from the contact surface, was again reflected from the wall, etc. Thus, a series of shock waves of decreasing amplitude, passed through the boundary, and alternatively accelerated and slowed down the boundary in pulsed and jumpwise manner. The flow picture was registered by an IAB-451 shadow instrument combined with a high-speed SFR moving-image camera operating in the time-magnifier mode. The result of each experiment was a series of Schlieren photographs for different instants of time.

The experimental results show that immediately after the start of the motion the boundary becomes distorted, as a result of the instability,<sup>[5,6]</sup> under the influence of small-scale perturbations that increase with time. The initial cause of the perturbation is made up of the following:

a) irregular pressure perturbations in the shock wave, as a result of the non-one-dimensional character of the rupture of the diaphragm of the shock tube and the diffraction of the shock wave by irregularities on the shock-tube wall.

b) small-scale wrinkles and variations in the film thickness ( $\pm 50\%$  of the average thickness).

The boundary perturbations gradually smear out to form a turbulent zone that increases with time and has uneven edges. Figure 2 shows, for the instant of time  $t = 700$   $\mu$ sec after the start of the boundary motion, a Schlieren photograph of the zone of turbulent mixing on the air-helium boundary (a), and a photograph of a control experiment in which air was present on both sides of the film (b). Here 1—zone of turbulent mixing, 2—

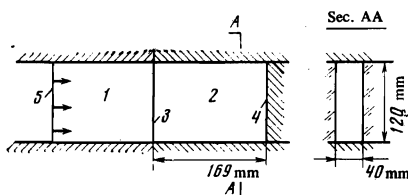


FIG. 1.

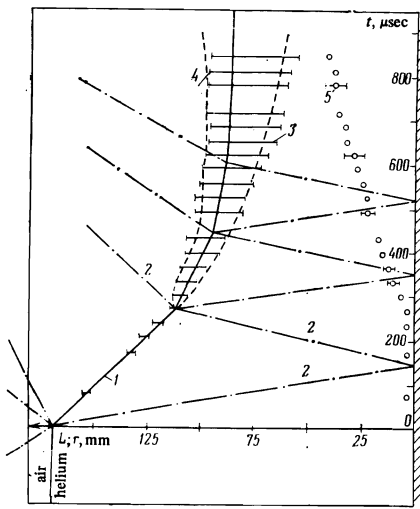


FIG. 3.

film, 3—rigid wall at end of channel 4—structure elements located outside the tube channel, and 5—“loop” (see below). In photograph 2a the zone of turbulent mixing has a cellular structure typical of Schlieren photographs of turbulent flows (see, e.g., [7]). The control experiment (Fig. 2b) does not show turbulent mixing, and the film moves as a unit with slight distortions.

The results of the measurement of the position of the zone of turbulent mixing and of its width  $L$  in one of the experiments, and the calculated  $r-t$  flow diagram ( $r$  is the distance from the rigid wall) are shown in Fig. 3. Here 1—boundary, 2—shock waves (calculated); 3, 4, — front and rear boundaries of the turbulent mixing zone; 5— $L \sim L(t)$ . The data of Fig. 3 show that the zone of turbulent mixing broadens asymmetrically relative to the calculated position of the boundary. In the initial stage ( $t \approx 300 \mu\text{sec}$ ) the value of  $L$  increases at an accelerated rate. The acceleration of the growth of the zone of turbulent mixing through which a shock wave passes can be attributed to the following factors: a) instability of the type considered in [5,6]; b) generation of vortices under situations when the shock wave passes through regions having a density gradient in a direction normal to the direction of motion of the shock wave; c) passage of the shock wave through a light inclusion in the heavier gas, or conversely, by the fact that this inclusion is accelerated to a velocity larger (smaller) than the mass velocity of the surrounding gas.

The presence of the film cannot influence to any extent the dynamics of the motion as a whole, in view of its relatively small mass, but does apparently influence the development of the zone of turbulent mixing. One can therefore not exclude the need for refinements of the foregoing measurement results, namely, the film may exert a stabilizing influence in the initial stage of motion, and in the later stage ( $t \approx 900 \mu\text{sec}$ ), the estimated mass of the pieces of film mixed with the zone of turbulent mixing amounts to only 1.5–2% of the film, but these pieces can serve as an additional source of perturbations and contribute to the growth of the zone of turbulent mixing.

Let us note one more peculiarity. The edge of the

turbulent mixing zone remains at the channel walls in the form of a “loop” (Fig. 2a). The presence of the “loop” under certain conditions may make it difficult to visualize the rear boundary of the turbulent mixing zone.

### 3. NUMERICAL CALCULATIONS OF THE INSTABILITY OF THE CONTACT SURFACE AND COMPARISON OF THE CALCULATIONS WITH EXPERIMENT

The system of Eqs. (1)–(5) together with (6) or (7) was solved numerically on the basis of the two-dimensional procedure described in [9], by the method of separation on the basis of the physical processes.<sup>1)</sup> The experiment described above was calculated numerically. We used Eq. (6) for  $v_t$ . The geometry of the calculation was similar to the experimental one and is shown in Fig. 1. On the left boundary we specified a constant pressure  $P_0$  such that a shock wave with a Mach number  $M = 1.3$  was produced. The boundary condition on the right was the presence of the rigid wall. The substances were regarded as ideal gases with parameters corresponding to a pressure  $P = 1 \text{ atm}$  and to  $T = 20^\circ \text{C}$ . The programs for calculating the turbulent mixing were turned on at  $t = 200 \mu\text{sec}$ . The constants used in the calculations were  $k_1 = 0.4$ ,  $k_2 = 0$ , and  $S_e = 0.5$ . These values of the constants are of the same order as the experimental values obtained in experiments on flow with shear and over a boundary layer. The value of  $\alpha$  in (6) was chosen such as to obtain the best agreement between the zone width and experiment. This value turned out to be 0.10. A close value of  $\alpha$ , obtained on the basis of an analysis of the experiments on stationary flow, was used in [1]. Figure 3 shows the  $r-t$  diagrams of the separation boundary between air and helium (solid curve) calculated without mixing, the  $r-t$  diagrams of the shock waves (dash-dot), and the boundaries of the mixing zone (dashed) calculated by using a mixing value based on a 0.5% deviation of the air concentration from the initial value. Figure 4 shows profiles of the density (curve 1) and of the air concentration (curve 2) in the mixing zone at  $t = 660 \mu\text{sec}$ . It is seen from Fig. 3 that at  $\alpha = 0.10$  the agreement between calculation and experiment (the horizontal segments mark the width of the mixing zone) is satisfactory. Some deviations at the initial stage of the processes are most likely due to the fact that immediately after the passage of the first shock wave through the boundary one observes in the experiment not turbulent mixing but the growth of the initial perturbations.

We note in conclusion that the choice of the values of all the parameters that enter in the model, and the

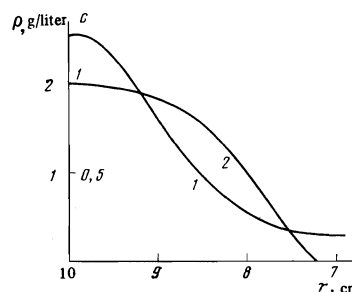


FIG. 4.

choice of the equation for  $\nu_t$ , can be made only after more complete experimental data on the structure of the mixing zone become available.

The authors thank V. Bashurin and V. Zhmailo for useful discussions.

<sup>1</sup>Turbulent mixing was introduced into the numerical calculations within the framework of the model of<sup>[1]</sup> by V. E. Neuvashaev and V. G. Yakovlev (Preprint No. 70, Inst. Appl. Math. USSR Acad. Sci., 1975).

<sup>1</sup>S. Z. Belen'kii and E. S. Fradkin, Tr. Fiz. Inst. Akad. Nauk SSSR 29, 207 (1965).

<sup>2</sup>M. A. Levine, Phys. Fluids 13, 1166 (1970).

<sup>3</sup>A. A. Pavel'ev, Izv. Akad. Nauk SSSR, Mekh. Zhidk Gaz.

No. 1, 38 (1974).

<sup>4</sup>A. N. Sekundov, *ibid.* No. 5, 114 (1971).

<sup>5</sup>E. E. Meshkov, *ibid.* No. 5, 151 (1969).

<sup>6</sup>R. D. Richtmeyer, Commun. on Pure and Appl. Math. 13, 297 (1960).

<sup>7</sup>N. F. Derevyanko and A. M. Trokhan, Zh. Prikl. Mekh. Teor. Fiz. No. 4, 105 (1968).

<sup>8</sup>G. Rutinger and L. M. Somers, J. Fluids Mech. 7, 161 (1960).

<sup>9</sup>M. Batalova, S. Bakhrakh, O. Vinokurov, V. Zaguskin, L. Ivanova, A. Kalmanovich, and I. Sinderman, Tr. Vsesoyuznogo seminara po chislennym metodam mekhaniki vyazkoi zhidkosti (Proc. All-Union Seminar on Numerical Methods of Mechanics of a Viscous Liquid), Nauka, Novosibirsk, 1969, p. 283.

Translated by J. G. Adashko

## Dependence of the magnetic moment of a layer magnet on the magnetic field

S. B. Khokhlachev

L. D. Landau Theoretical Physics Institute, USSR Academy of Sciences

(Submitted March 25, 1976)

Zh. Eksp. Teor. Fiz. 71, 812-815 (August 1976)

The dependence of the magnetic moment of a layer magnet on the magnetic field is found in the leading logarithmic approximation.

PACS numbers: 85.70.Nk

The magnetic-moment measurements of<sup>[1]</sup> show that in layer magnets with ferromagnetic intraplanar interaction and weak anisotropy there is a region of fields in which the moment is a linear function of the logarithm of the external magnetic field. At the same time, the explanation of this fact, based on the spin-wave approximation, cannot be regarded as satisfactory, since this approximation is not valid in the two-dimensional case. It has been shown by Polyakov<sup>[2]</sup> that in the two-dimensional case the interaction of spin waves turns out to be extremely important and determines the dependence of the physical quantities on the logarithm of the characteristic lengths (in<sup>[2]</sup> the question of the behavior of the correlation functions was considered). He also proposed a method of summing the leading logarithmic terms of the low-temperature expansion. Here we shall apply this method to determine the dependence of the magnetic moment on the external magnetic field.

In the problem under consideration there are several characteristic lengths: first, the correlation length  $R_c$  due to the magnetic field; secondly, the length scale associated with the intraplanar anisotropy; thirdly, the distance between the layers in which the magnetic atoms are situated, and, finally, the distance  $a$  between magnetic atoms in the plane. The magnetic moment has different dependences on the external field, depending on the relative sizes of these length scales (cf. <sup>[3]</sup>). The results of the work of Pokrovskii and Uimin<sup>[3]</sup> pertain to the case of very weak fields, when the correlation length due to the magnetic field is much larger than the

length scale associated with the intraplanar anisotropy. In this paper we consider the case of sufficiently strong fields (the criterion will be given below), which are, nevertheless, much smaller than the saturation field.

In the following we shall consider a generalized Heisenberg model with an  $N$ -component "spin." We shall call the generators of the group of rotations in  $N$ -dimensional space a spin operator (in the Heisenberg model,  $N=3$ ). We shall be interested in the dependence of physical quantities on the logarithm of the magnetic field, and therefore we can neglect the noncommutativity of the spin operators and the difference between lattice sums and integrals. The problem of calculating the thermodynamic averages then becomes classical, and it is necessary to replace the spin operators by  $N$ -component unit vectors. The Heisenberg Hamiltonian then acquires the form

$$\mathcal{H} = \frac{1}{2} J \int d^2x [(\partial_\mu n)^2 - 2a^{-2} B n(x)], \quad (1)$$

where  $J$  is the exchange integral,  $B$  is the external magnetic field,  $n$  is a unit  $N$ -component vector, and  $a$  is the distance between magnetic atoms in the lattice. In (1) we have neglected the interplanar interaction and the anisotropy. It can be seen from the Hamiltonian (1) that the correlation length is related to the magnetic field:  $R_c = a(J/B)^{1/2}$ .

We define the magnetic moment  $M$  by the formula